Mathematical Modeling and Kinetic Study of Deep Hydrodesfulfurization of Dibenzothiophenes Using CoMoP/Al_2O_3 Catalyst

Ana L.O. Silva[1]*, José Faustino F.S. Filho[1], Roymel R. Carpio[1], Mônica A.P. Silva[1], Argimiro R. Secchi[2]
[1]Chemistry School; Universidade Federal do Rio de Janeiro; [2]Chemistry Engineering Program, COPPE, Universidade Federal do Rio de Janeiro; Rio de Janeiro, Rio de Janeiro, Brazil

Deep hydrodesulfurization (HDS) is a highly effective process for removing sulfur from petroleum and its derivatives, achieving ultra-low sulfur levels, improving fuel quality, and reducing air pollution. This study estimates kinetic parameters for the HDS process using experimental data for dibenzothiophene (DBT) and 4,6-dimethyldibenzothiophene (4,6-DMDBT) on a CoMoP/Al_2O_3 catalyst in a fixed-bed reactor. A global power-law model provided the best fit for each dataset ($R^2 > 0.99$), while a single individual model was suitable across all data. The estimated reaction order concerning hydrogen was 0 for DBT and 1 for 4,6-DMDBT. Pre-exponential Arrhenius constants and activation energies (ranging from 90–100 kJ/mol) were also estimated and can be applied to reactor design and process optimization in HDS systems.

Keywords: Deep Hydrodesulfurization Reaction. CoMoP/Al_2O_3. Kinetic Modeling. Dibenzothiophene. 4,6-Dimethyldibenzothiophene.

Air pollution and the environmental impact caused by high sulfur emissions from fossil fuels are pressing global concerns. When sulfur-containing fuels are combusted, sulfur dioxide (SO_2) is released into the atmosphere, forming acid rain. SO_2 is also toxic, corrosive, and detrimental to infrastructure and ecosystems. Furthermore, nitrogen oxides formed during combustion exacerbate air pollution and pose severe risks to human health [1].

In Brazil, the transport sector accounts for 33% of primary energy consumption, relying heavily on diesel due to the predominance of road transport, as shown in Figure 1. To mitigate emissions, stricter regulations have been implemented, including ultra-low sulfur diesel (ULSD) standards. ANP Resolution No. 968/2024 mandates a maximum sulfur content of 10 ppm (S-10 diesel) in urban areas, while rural regions still utilize S-500 diesel, containing up to 500 ppm of sulfur. Since 2013, the use of S-10 diesel has significantly increased, currently comprising 60% of national diesel production. A complete transition to S-10 is projected within the next decade [2]. However, achieving this goal requires improved efficiency in petroleum product hydrotreatment (HDT) units. HDT is essential for purifying feedstocks and removing contaminants through hydrogenation reactions, among which hydrodesulfurization (HDS) is specifically responsible for sulfur removal.

Hydrodesulfurization (HDS)

Although the HDS process is well established, achieving ultra-low sulfur levels through deep HDS remains challenging due to the complexity of

Figure 1. Fuel Consumption in Brazil.

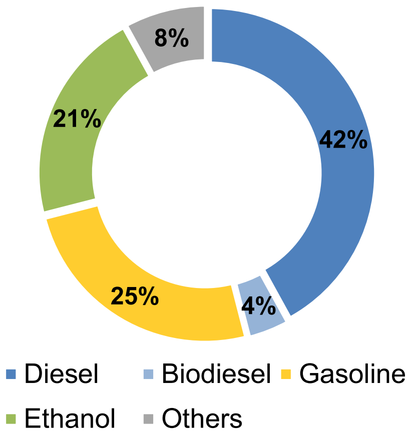

Received on 28 January 2025; revised 12 March 2025.
Address for correspondence: Ana Silva. Av. Athos da Silveira Ramos, 149 - Cidade Universitária, Rio de Janeiro - RJ, Brazil. Zipcode: 21941-909. E-mail: analuiza.os@eq.ufrj.br.

J Bioeng. Tech. Health 2025;8(2):188-195

fuel compositions and the simultaneous removal of other contaminants. Many compounds present in the feedstock or formed during HDT reactions compete for the catalyst's active sites, thereby reducing HDS reaction rates. Nitrogen-containing compounds, in particular, inhibit the reaction by adsorbing onto the catalyst surface and delaying hydrogen activation. Additionally, coke formation, promoted by heterocyclic nitrogen compounds, significantly shortens catalyst life [3].

Modeling HDS is complex but vital for optimizing process conditions, maximizing sulfur removal efficiency, and minimizing costs. Hydrogen, a key input in this process, typically supplied in excess to increase conversion, often represents the second-highest operational cost in refineries [4]. Improving process efficiency enhances sulfur removal and reduces energy and material costs. Therefore, accurate modeling of deep HDS reactions is critical for meeting S-10 diesel production goals.

Among the primary sulfur-containing compounds in diesel, dibenzothiophene (DBT) and 4,6-dimethyldibenzothiophene (4,6-DMDBT) are recognized as the most refractory. As shown in Figure 2, both compounds transform two parallel reaction pathways. In the direct desulfurization (DDS) route, DBT and 4,6-DMDBT produce hydrogen sulfide (H_2S) and biphenyl (BPH), leading to products such as cyclohexylbenzene (CHB) or 3,3’-dimethylbiphenyl (3,3’-DMBPH). In the hydrogenation (HYD) route, DBT undergoes hydrogenation of one of its aromatic rings to form an equilibrium mixture of tetrahydrodibenzothiophene (THDBT) and hexahydrodibenzothiophene (HHDBT), which are rapidly converted to CHB. For 4,6-DMDBT, the hydrogenation pathway yields products such as methyl cyclohexyl toluene (MCHT) or dimethyl cyclohexane (DMBCH) alongside H_2S [5].

Materials and Methods

Figure 3 shows the steps taken to achieve the research objective.

Development of the Parameter Estimation Procedure

The selected mathematical models were implemented using the Environment for Modeling, Simulation, and Optimization (EMSO) software [6], employing the EML (EMSO Modeling Library), an open-source modeling language. The resulting systems of algebraic differential equations from the predefined models were solved using a multi-step integration method with the DASSLC integrator [7], applying relative and absolute tolerances of 10^{-6} and 10^{-8}, respectively.

Parameter estimation was performed using the Nelder and Mead flexible polyhedron optimization method, with relative tolerances of 10^{-6} for both the objective function and the estimated parameters [8]. The global optimum was ensured by initializing the optimization procedure from multiple starting points within the predefined lower and upper parameter bounds.

The parameter estimation results were subjected to statistical evaluation using tests integrated into EMSO, including the Student's t-test and Fisher's F-test, both conducted at a 95% confidence level. The Chi-square test was also employed to assess the goodness-of-fit of the estimated models concerning the objective function value.

Kinetic Models

For the formulation of mass conservation equations, the reactions were considered irreversible. The hydrogen was assumed to be in excess, and the catalyst bed was modeled as isothermal. The hydrogen concentration in the liquid phase and the maximum degree of vaporization of the solvents and reactants were estimated for each experimental condition. A flash calculation that employed the Soave-Redlich- Kwong equation of state to represent all components in the feed mixture were used in HYSYS do determine these parameters.

In accordance with existing literature [3], power-law models were selected to describe the

Figure 2. HDS Reaction scheme for DBT and 4,6-DMDBT.

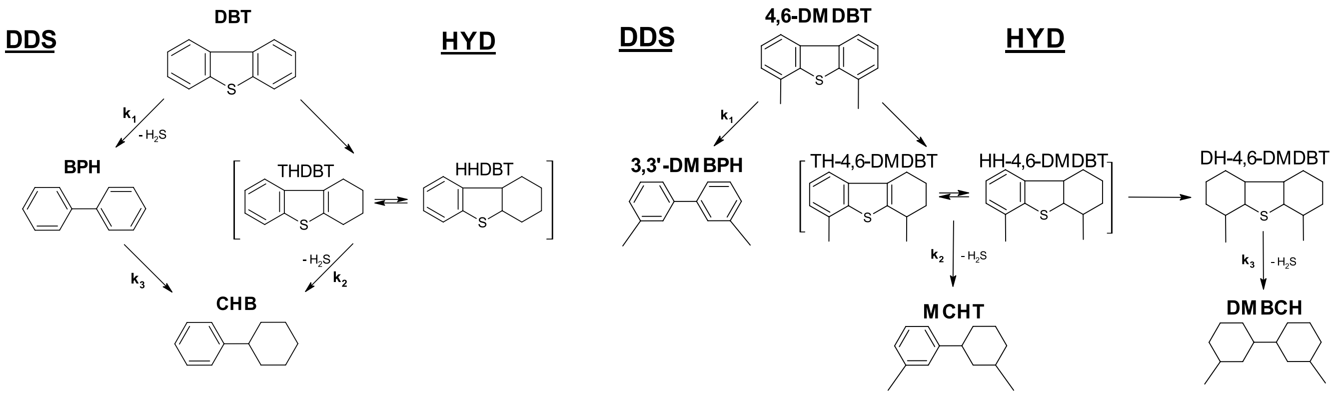

Figure 3. Method flowchart.

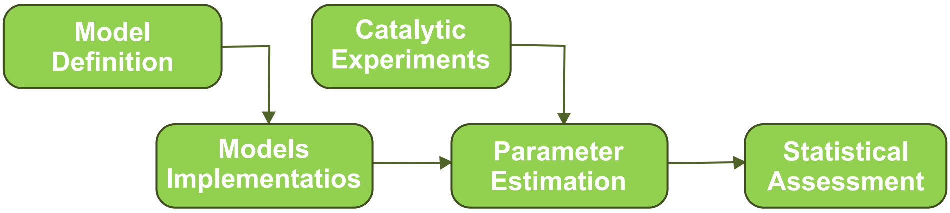

reaction rate, as shown in Table 1. Global models were used to evaluate the overall behavior of the HDS process and the conversion of sulfur-containing reactants. Meanwhile, individual models (Table 2) were developed to investigate the detailed reaction mechanisms and the intermediate and final product formation rates in each pathway.

To minimize parameter correlation during estimation, the kinetic parameters were reparameterized using a modified Arrhenius equation with a reference temperature (T_{ref}), as proposed by Schwaab and colleagues [9]:

$$k\ (T) = k_0 exp\left(-\frac{E_a}{RT}\right) = exp\left[-a + b\left(1 - \frac{T_{ref}}{T}\right)\right]$$

In this formulation, the pre-exponential factor (k_0) and activation energy E_a are replaced by the estimation parameters *a* and *b*, respectively. This transformation expresses the explicit temperature dependence of the reaction rate while reducing parametric correlation in the optimization procedure.

Catalytic Experiments

Initially, the procedure outlined in Section "Development of the Parameter Estimation Procedure" was validated using experimental data from previous studies conducted by the Laboratory for Development of Catalytic Processes (LDPC) [3]. These data were based on DBT, the model refractory compound, using a $CoMoP/Al_2O_3$ catalyst. Subsequently, new catalytic tests were carried out using 4,6-DMDBT, a more refractory compound, to investigate further the kinetic behavior under the technological challenge addressed in this study.

For both feedstocks, the experimental procedure followed the same protocol. The catalyst bed underwent two-step sulfidation with a 4 wt% carbon disulfide solution in *n*-hexane at a flow rate of 0.10 mL/min prior to reaction testing. All experiments were conducted in a fixed-bed reactor (PID Eng & Tech) operated in up-flow mode. Initial sulfur concentrations were 3500 mg/kg for DBT and 1000 mg/kg for 4,6-DMDBT, with *n*-hexadecane

Table 1. Global models evaluated in this work.

Name	Acronym	Models	
		DBT	4,6-DMDBT
Pseudo first Order Global Power Law	PGP	$r_{HDS} = kC_{DBT}$	$r_{HDS} = kC_{4,6-DMDBT}$
Second Order Global Power Law	SGP	-	$r_{HDS} = kC_{4,6-DMDBT}C_{H_2}$
Variable Orders Global Power Law	VGP	$r_{HDS} = kC_{DBT}^{\alpha}\ C_{H_2}^{\beta}$	-

Table 2. Individual models evaluated in this work.

Name	Acronym	Models	
		DBT	4,6-DMDBT
Individual Powers Law	IP	$r_{DBT} = -k_1C_{DBT} - k_2C_{DBT}C_{H_2}$ $r_{BPH} = k_1C_{DBT} - k_3C_{BPH}C_{H_2}$ $r_{CHB} = k_2C_{DBT}C_{H_2} + k_3C_{BPH}C_{H_2}$	$r_{4,6-DMDBT} = -k_1C_{4,6-DMDBT} - k_2C_{4,6-DMDBT}C_{H_2}$ $r_{3,3-DMBPH} = k_1C_{4,6-DMDBT}$ $r_{MCHT} = k_2C_{4,6-DMDBT}C_{H_2} - k_3C_{MCHT}C_{H_2}$ $r_{DMBCH} = k_3C_{MCHT}C_{H_2}$
Parallel Individual Power Law	PIP	$r_{DBT} = -k_1C_{DBT} - k_2C_{DBT}C_{H_2}$ $r_{BPH} = k_1C_{DBT}$ $r_{CHB} = k_2C_{DBT}C_{H_2}$	$r_{4,6-DMDBT} = -k_1C_{4,6-DMDBT} - k_2C_{4,6-DMDBT}C_{H_2}$ $r_{3,3-DMBPH} = k_1C_{4,6-DMDBT}$ $r_{MCHT} = k_2C_{4,6-DMDBT}C_{H_2}$

as the solvent. The gas-to-oil ratio was maintained at 400 (NL/L). Reaction progress was monitored using gas chromatography (Agilent 6890 N). The mass balance closure exceeded 95% for all experimental conditions and catalysts. The reactor achieved steady-state operation after approximately 5 hours for DBT and 7 hours for 4,6-DMDBT, with less than 2.0% conversion variations.

Experimental error was assessed through replicate measurements for each model compound. The operating conditions—temperature, pressure, and weight hourly space velocity (WHSV)—for the reference DBT dataset followed a three-level factorial design comprising 27 experiments. For 4,6-DMDBT, a partial factorial design of six experimental conditions was selected, matching the same variables. This subset was intended as a foundation for a sequential design to expand the parameter estimation dataset in the second phase. Table 3 presents the extreme values of each variable in the design.

The experimental error of the complete factorial design was calculated using the replica condition, which is the central point of all variables. The conditions for the partial planning were chosen to obtain information from the variable bounds and provide a well-distributed range of conversions. In this case, the conditions used to calculate the experimental and replication error were Temperature = 270 ºC, WHSV = 60 h^{-1}, and P = 60 bar.

Results and Discussion

Two global models were found to have acceptable adjustments ($R^2 > 0.99$) and statistical significance. Figure 4 show the model adjustment graphs for DBT and 4,6- DMDBT reagent concentration data, and Tables 4 and 5 show the results of parameter estimation.

The order for data with DBT was 0.4 ± 0.2 concerning the sulfur compound and zero concerning hydrogen. For 4,6-DMDBT, a global second-order model with an order of 1 concerning each reactant was the most appropriate. This parameter indicates whether the relevant step for

Table 3. Factorial planning conditions for experiments with each compound.

Variable	DBT		4,6-DMDBT	
	Minimum Value	Maximum Value	Minimum Value	Maximum Value
Temperature (°C)	210	270	240	300
Pressure (bar)	30	60	30	60
WHSV (h^{-1})	4	8	8	14

Table 4. Estimation results for global model with DBT.

Model	Parameter	Result
VGP	α	0.4 ± 0.2
	β	Not statistically significant
	a	5.0 ± 0.7
	b	24.1 ± 3.1
	E_a	86.3 ± 11.2
	$\ln k_0$	29.2 ± 3.8
	F_{obj}	24.2
	R^2	0.9902

Table 5. Estimation results for global model with 4,6-DMDBT.

Model	Parameter	Result
SGP	a	-2.7 ± 0.1
	b	19.6 ± 2.8
	E_a	88.6 ± 12.4
	$\ln k_0$	22.3 ± 2.7
	F_{obj}	15.2
	R^2	0.9948

Figure 4. Predicted *versus* observed concentrations for Global Models with DBT and 4,6- DMDBT, respectively.

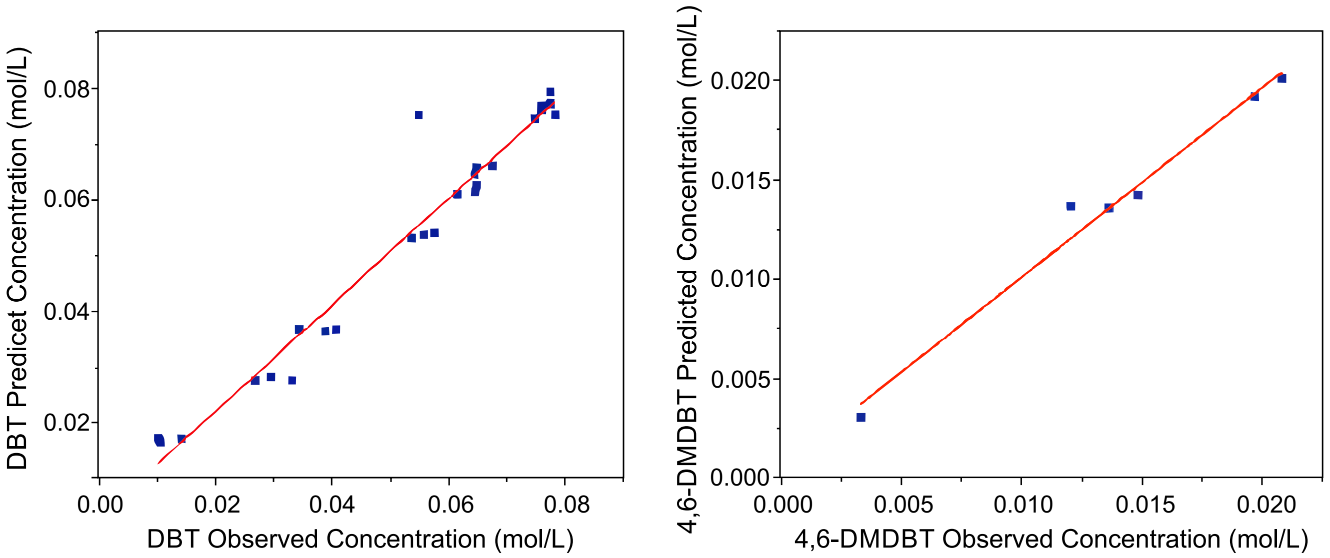

the reaction kinetics depends on hydrogen. The results indicate that DDS was the preferred route for the first compound, while for the second, it was HYD, as established in the literature [5]. In the individual models, the same model (PIP) presented acceptable fits ($R^2 > 0.98$), as shown in Figure 5 and parameters with statistical significance in Tables 6 and 7.

Figure 6 clearly shows that, despite the same models, the preferred routes for each representative compound have been inverted. The figure shows the rate of each product calculated by the models in the same temperature range (240 to 270°C). The formation rate of BPH and MCHT is higher than that of CHB and 3,3'-DMBPH, which corroborated the precedent that DDS was the dominant route for DBT, while 4,6-DMDBT predominantly followed the HYD pathway.

Conclusion

The evaluated kinetic models agreed well with the experimental data and yielded statistically significant parameters. Apparent activation

Figure 5. Predicted *versus* observed concentrations for Individual models with DBT and 4,6- DMDBT, respectively.

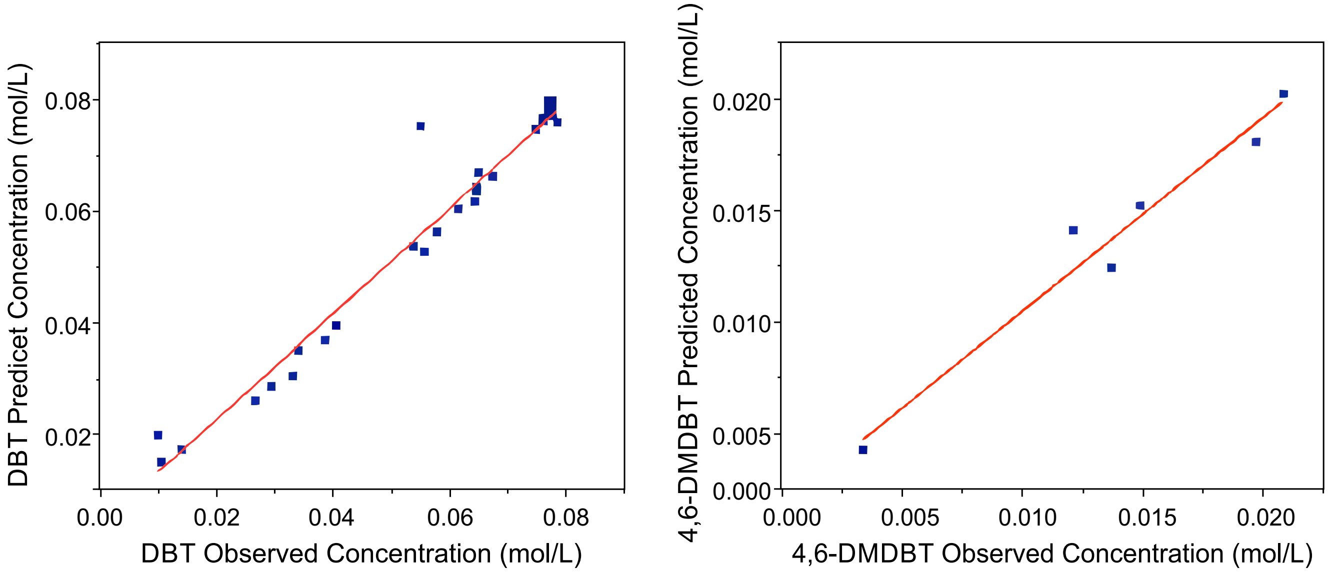

Table 6. Estimation results for best individual model with DBT.

Model	Parameter	Result
PIP	a_1	-1.5 ± 0.1
	b_1	22.7 ± 2.3
	E_{a_1}	100.5 ± 10.2
	$\ln k_{o_1}$	21.2 ± 2.4
	a_2	-1.7 ± 0.1
	b_2	22.7 ± 2.9
	E_{a_2}	101.3 ± 12.9
	$\ln k_{o_2}$	21.0 ± 3.0
	F_{obj}	89.9
	R^2	0.9884

Table 7. Estimation results for best individual model with 4,6-DMDBT.

Model	Parameter	Result
PIP	a_1	-0.6 ± 0.3
	b_1	19 ± 7
	E_{a_1}	87.6 ± 31.5
	$\ln k_{o_1}$	20.0 ± 6.7
	a_2	-2.1 ± 0.1
	b_2	19 ± 3
	E	85.5 ± 13.9
	$\ln k_{o_2}$	21.1 ± 3.0
	F_{obj}	180.2
	R^2	0.9843

Figure 6. Comparison of the product formation rate as a function of the reagent consumption rated.

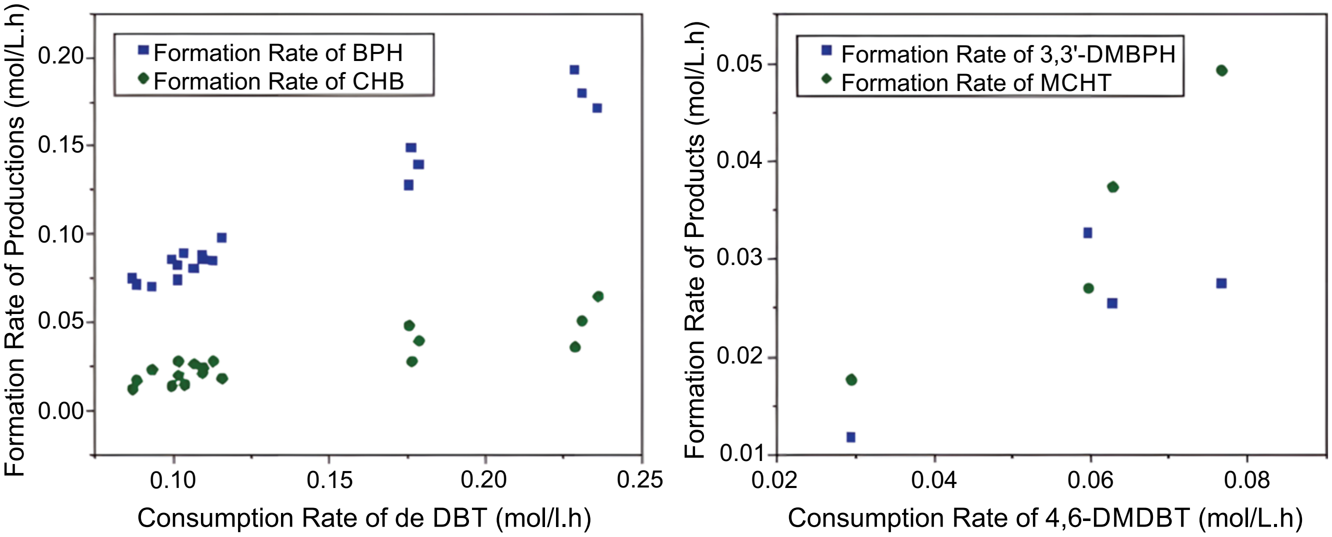

energies were estimated in the 90–100 kJ/mol range, consistent with values reported in the literature. The more refractory nature of 4,6-DMDBT compared to DBT was confirmed by the need for a higher operating temperature range (240–300 °C for 4,6-DMDBT *vs.* 210–270 °C for DBT) to achieve similar conversion levels. The best-fitting global models highlighted differences in the estimated reaction order concerning hydrogen: 0 for DBT and 1 for 4,6-DMDBT. Likewise, the individual models enabled accurate predictions of product formation rates, showing the faster formation of biphenyl (BPH) for DBT and methyl cyclohexyl toluene (MCHT) for 4,6-DMDBT.

These findings reinforce the preference for different reaction pathways—DDS for DBT and HYD for the more refractory 4,6-DMDBT. These insights facilitate the adjustment of key operational parameters, such as temperature, pressure, and WHSV, for known refractory diesel feeds. They also support more accurate reactor design and process optimization to achieve ultra-low sulfur concentrations via hydrodesulfurization (HDS), ultimately enhancing fuel quality and reducing air pollution.

The next step involves conducting a sequential experimental plan to evaluate and estimate kinetic parameters for competitive reactions involving 4,6-DMDBT and nitrogen-containing compounds. This will yield a more realistic representation of refinery feed compositions while increasing laboratory efficiency through focused experimentation and more statistically robust parameter estimation.

Acknowledgments

The authors gratefully thank Agência Nacional do Petróleo, Gás Natural e Biocombustíveis – ANP – and Financiadora de Estudos e Projetos - FINEP - through the ANP's Programa de Recursos Humanos for the Natural Gas and Biofuels Sector - PRH-ANP. In particular, PRH/ANP 3.1 – Programa de Recursos Humanos para Capacitação em Processos e Sistemas da Indústria de Petróleo e de Biocombustíveis – for financial support. Mônica A. P. Silva acknowledge Fundação de Amparo à Pesquisa do Estado do Rio de Janeiro - FAPERJ – and Conselho Nacional de Desenvolvimento Científico e Tecnológico – CNPq – for financial support.

References

1. Muro AJ. Política, sistemas normativos e instrumentos de controle da poluição do ar: aspectos legais. SJRJ. 2014;21(41):19-49. Available from: https://www.jfrj.jus.br/sites/default/files/revista-sjrj/arquivo/PDF_0.

2. Empresa de Pesquisa Energética – EPE; Ministério de Minas e Energia – MME. Plano Decenal de Expansão de Energia 2032. Rio de Janeiro: EPE/MME; 2022. Available from: https://www.epe.gov.br/pt/publicacoes-dados-abertos/publicacoes/plano-decenal-de-expansao-de-energia-2032.
3. Nascimento IG, Locatel WR, Magalhães BC, Travalloni L, Zotin, Silva MAP. Kinetics of dibenzothiophene hydrodesulfurization reactions using CoMoP/Al_2O_3 and NiMoP/Al_2O_3. Catal Today. 2021;381:200-208.
4. Jiao Y, Su H, Hou W, Liao Z. Optimization of refinery hydrogen network based on chance constrained programming. Chem Eng Res Des. 2012;90:1553-1567.
5. Mello MD, Braggio FA, Magalhães BC, Zotin JL, Silva MAP. Kinetic modeling of deep hydrodesulfurization of dibenzothiophenes on NiMo/alumina catalysts modified by phosphorus. Fuel Process Technol. 2018;177:66-74.
6. Soares RP, Secchi AR. EMSO: A new environment for modelling, simulation and optimization. Comput Aided Chem Eng. 2003;14:947-952.
7. Secchi AR. DASSLC v3.9 - Differential-Algebraic System Solver in C [Internet]. Porto Alegre: Universidade Federal do Rio Grande do Sul; 2012. Available from: http://www.enq.ufrgs.br/enqlib/numeric.
8. Nelder JA, Mead R. A simplex method for function minimization. Comput J. 1965;7:308-313.
9. Schwaab M, Pinto JC. Optimum reference temperature for reparameterization of the Arrhenius equation. Part 1: Problems involving one kinetic constant. Chem Eng Sci. 2007;62:2750-2764.